Atomistic study of defects in $YBa_2Cu_3O_7$

Roger C. Baetzold
Corporate Research Laboratories, Eastman Kodak Company, Rochester, New York 14650-2001
(Received 30 November 1989; revised manuscript received 9 March 1990)

The orthorhombic structure of $YBa_2Cu_3O_7$ has been described in terms of the shell model and associated two- and three-body short-range interaction potentials. The empirical potentials are determined by fitting the structure and experimental elastic-constant values. These potentials are used to compute point-defect energies and small-polaron energies. An oxidation reaction of Cu^+ and lattice oxygen ions leading to O^- is shown to be probable. Migration energies of oxygen ions by a vacancy mechanism near the Cu-O plane have a computed activation energy on the order of 0.3 eV. Phonon frequencies are computed from the potentials and shown to agree well with experimental Raman data. Bipolarons in the crystal are examined, and the species O_2^{2-} is shown to be rather stable.

INTRODUCTION

The copper oxide based high-temperature superconductor materials have a variety of solid-state properties that are being studied in order to better understand the mechanism of superconductivity.[1-3] While these various experimental studies progress, there develops a need to understand microscopic details of the crystal properties. This provides a basis for the application of simulation techniques to these materials. A number of atomistic simulation studies treating the superconductor as an ionic solid have appeared. These include studies of La_2CuO_4,[4,5] $YBa_2Cu_3O_7$,[6,7] some of the ternary cuprates[8,9] and Bi-containing materials.[10]

The simulation studies have been successful in determining a number of properties of the material. The first studies,[4,5] focusing on the La_2CuO_4 material, demonstrated a softening of an optic-phonon mode, which was later found experimentally.[11] In addition the possibility of bipolaron[4,5] formation either as a Cu^{3+}-Cu^{3+} or O_2^{2-} species was examined, and the latter was shown to be stable by a few tenths of an electron volt in this high dielectric material. This mechanism has been elaborated with the addition of spin pairing terms such as those discussed by de Jongh[12,13] in an exchange bipolaron mechanism of superconductivity.

We have developed an empirical potential model[6] that accurately reproduces the structure[14] of orthorhombic $YBa_2Cu_3O_7$. This empricial model utilizes various two-body oxide potentials used in earlier simulation studies[15-18] of metal oxides. This potential model has successfully been used to determine bipolaron and defect energies in the solid as well as determining compensation mechanisms and sites of impurity substitution within the crystal. While these studies have agreed quite well with experiment in terms of impurity site substitution, the potential model is subject to further refinement. In particular various recent experimental studies of elastic constants have provided evidence for a less stiff crystal structure than our first potential model predicted.[19,20] Thus we have undertaken the present studies to determine potentials which are softer but which remain stable throughout the Brillouin zone and give a good fit to structure of $YBa_2Cu_3O_7$. These potentials and their properties will be the subject of this report.

Various solid-state properties of the $YBa_2Cu_3O_7$ material are crucial to its behavior and amenable to study by our simulation techniques. An example is oxygen diffusion which is a temperature activated process. It is well known[21,22] that the superconducting transition temperature depends upon oxygen content. Oxygen diffusion during preparation in various ambient conditions thus becomes of importance. We will examine some mechanisms of oxygen diffusion which have been discussed in experimental studies[23-25] of this material. In addition the energetics of oxygen reactions with the crystal have been recently reported[26] and will be computed here. Bipolaron defect species including the peroxide O_2^{2-} species discussed in some models of the material will be examined.

METHOD

Details of the atomistic simulation method have been discussed in various reviews.[18,27,28] Nevertheless it has seemed generally advisable to review the formalism. An ionic description of the perfect crystal structure is the starting point. Thus ions are represented as having integer charges, but within the scope of the polarizable shell model.[29] Thus every ion has a shell and core representing its electron charge and polarization properties. The shell model harmonically couples the massless shell and core to determine the energy as a function of displacement. We should note that these Coulombic type interactions account for approximately 90% of a typical crystal's lattice energy. The other component is the short-range energy arising from the overlap of electron clouds and a van der Waals type of interaction. Thus, the two-body potential interactions are in the form of a Buckingham function

$$\phi(r_{ij}) = Ae^{-r_{ij}/\rho} - C/r_{ij}^6 , \quad (1)$$

where r_{ij} is the internuclear shell separation and A, ρ,

and C are the appropriate constants. In addition to two-body interactions, a three-body term

$$\phi_{ijk} = \tfrac{1}{2}k'(\theta - \theta_0)^2 \quad (2)$$

is considered in this work where k' is a constant and the θ, θ_0 terms are angles relating the three centers in question. Thus the perfect crystal is described with the framework of the preceding considerations. Phonon-dispersion curves for a potential may be computed through application of the classical equations of motion. The phonon frequencies are computed at several points spanning the Brillouin zone and real values are indicative of a stable potential.

Defect energies are computed using the perfect crystal potential within a Mott-Littleton approach.[30] In this approach the ion cores and shells immediately surrounding a defect are allowed to relax and polarize explicitly. The response of more distant ions is treated by continuum approximations. The center region consists of 225 ions where the whole potential is involved and an enclosing spherical region of up to six lattice constants in radius where harmonic terms in the potential are involved. This methodology is embodied in the HADES III (Ref. 31) and CASCADE (Ref. 32) set of computer codes which we employ in this work. These codes not only compute the defect energies and ion positions, but give the perfect crystal elastic and dielectric constants.

Our potential for $YBa_2Cu_3O_7$ first involves specification of the charge states of the various ions. Clearly Y and Ba ions are 3+ and 2+, respectively, in this classical representation. Various distributions of charge on Cu and O ions deviating from the expected charges of ± 2.0 were examined in order to achieve neutrality in the formula unit. These include (i) all Cu 2.33+; (ii) all O, 1.86−; (iii) chain Cu, 3+ with plane Cu, 2+; and (iv) O ions attached to Cu chain as 1.67−. The latter description gave the most successful representation of the crystal structure while maintaining stability of the structure. This result is also in accord with relative charge distributions computed in quantum-mechanical semiempirical treatments[33] of the material.

We note the difficulties encountered with the various types of potential. In the case of (i), the best fits to structure were accompanied by negative dielectric constants. In the case of (ii), the fit to structure was poor and this gave a potential which was unstable when defects were introduced. In the case of (iii), stable potentials were found which gave reasonable structural fits and reasonable properties. This model, however, is at odds with most photoemission studies which do not observe Cu^{3+} and so we will not report data on this potential model. Thus, we are left with case (iv) which we will show is stable and gives good structural fit and reasonable properties. Of course some combinations of the four extreme cases which we studied might be worthy of investigation, but this would be an enormous task unless experimental information existed to select a particular case.

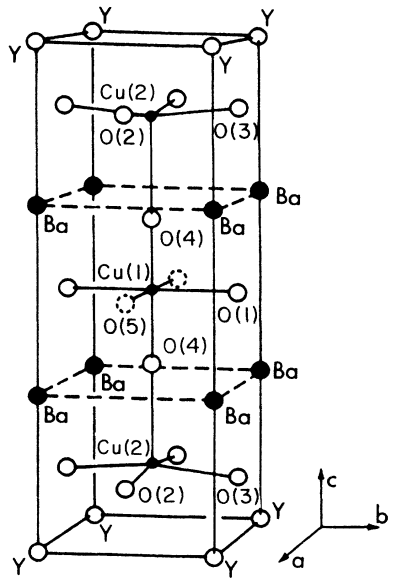

FIG. 1. Unit cell of the orthorhombic $YBa_2Cu_3O_7$ studied in this work.

In our procedure for developing a potential for $YBa_2Cu_3O_7$ we begin with potential interactions such as O-O and Ba-O, which are known from other studies[15,16] in metal oxides. The additional interactions are treated first by an electron-gas[34] representation. Usually at this point the structure is not well reproduced, and further fitting by variation of the parameters in the potentials is needed. When elastic constants or dielectric constants are available the procedure can be adjusted to fit to them

TABLE I. Comparison of experimental and calculated bond lengths in $YBa_2Cu_3O_7$ for the potentials used in this work.

Bond	Experimental	Potential 1	Potential 2	Potential 3
Cu(1)—O(1)	1.94	1.931	1.948	1.940
Cu(1)—O(4)	1.847	1.882	1.863	1.851
Cu(2)—O(2)	1.926	1.925	1.913	1.932
Cu(2)—O(3)	1.957	1.948	1.963	1.957
Cu(2)—O(4)	2.299	2.202	2.347	2.300
Ba—O(1)	2.883	2.867	2.921	2.872
Ba—O(4)	2.740	2.727	2.737	2.741
Ba—O(2)	2.964	2.925	2.995	2.979
Ba—O(3)	2.944	2.910	2.962	2.968
Y—O(2)	2.407	2.411	2.420	2.418
Y—O(3)	2.381	2.392	2.379	2.394

TABLE II. Computed[a] properties of various potentials.

Property	Potential 1	Potential 2	Potential 3
C_{11}	32.58	21.68	24.40
C_{12}	19.92	14.13	12.02
C_{13}	10.35	10.28	10.50
C_{33}	20.08	12.77	15.84
C_{44}	6.18	6.20	5.91
C_{66}	18.14	13.41	13.73
ϵ_0	17.37	36.50	14.81
ϵ_0	12.72	43.55	19.00
ϵ_0	19.57	38.83	12.64
ϵ_∞	6.44	3.71	3.66
ϵ_∞	5.38	3.64	3.58
ϵ_∞	4.83	3.17	3.18

[a]The units of the elastic constants C_{ij} are 10^{11} dyn/cm^2. The dielectric constants at low frequency ϵ_0 and high frequency ϵ_∞ are given successively in the a,b,c directions.

as well. We fit to the structure of $YBa_2Cu_3O_7$ determined by neutron diffraction.[14]

The unit cell of the orthorhombic $YBa_2Cu_3O_7$ studied in this work is shown in Fig. 1. We employ the site notation used earlier.[6] The comparison of experimental bond lengths with the corresponding equilibrium bond lengths for each potential is shown in Table I. The fits are quite good and generally the Cu_2-O_4 distance is reproduced with poorest accuracy. Potential 3 gives the best fit with maximum deviation from experiment of 0.02 Å.

An important consideration in developing a potential model is the computed elastic constants and how well they match experiment. Our crystal model contains seven oxygen ions per formula unit and corresponds to a temperature of 0 K. Experiment is typically carried out on samples which may be polycrystalline or small single crystal and the oxygen content may deviate from seven per formula unit. Thus some caution is necessary in comparing theory with experiment. Studies of the bulk moduli[35,36] and various elastic constants[37,38] have been reported for polycrystalline materials using ultrasonic techniques. The bulk moduli reported in these studies is smaller than our calculations from a prior potential,[6] although some x-ray diffraction measurements[39,40] do report comparable values. Recently Brillouin scattering studies[19] have been performed for small single crystals at 300 K having nearly O_7 stoichiometry. The values determined from this study are $C_{11}=21.1$, $C_{33}=15.9$, and an estimate of $C_{44}=3.3$ each in units of 10^{11} dyn/cm^2. In addition an inelastic neutron-scattering study[20] on small single crystals has been analyzed by a lattice dynamical model. This study gave the values $C_{11}=23.0$, $C_{33}=15.0$, $C_{44}=5.0$, $C_{66}=8.5$, $C_{12}=10.0$, and $C_{13}=10.0$ in units of 10^{11} dyn/cm^2. These experimental values may be compared to computed elastic constant data for our various potentials in Table II.

We have considered three new potentials in this work. Two are strictly two body in form while the other contains three-body bond harmonic forces.[41] The general strategy is to start with two-body potentials which are stable and then add the three-body terms so as to improve fit to structure and properties. Following this strategy we find that the most important bond bending term involves the O(1) and O(4) oxygen ions and two adjacent Ba ions. This was surprising, since it was expected that terms involving copper and oxygen ions would require three-body terms. Apparently the possible need for such terms, as would be expected for covalent bonds, is accounted for by the complex two-body interactions throughout the crystal.

The parameters in each potential are described in Table III. We note that potential 1 is just two body in form and has stable phonon frequencies throughout the Brillouin zone indicative of a stable potential. The structure fit is good, but in general the elastic constants are larger than the experimental data. Attempts to improve this fit within the two-body model give potentials with some instability by virtue of the appearance of imaginary phonon frequencies at the extremities of some parts of the Brillouin zone. Potential 2 displays this behavior. Potential 3 is our preferred model and has the inclusion of the three-body terms and fits structure and elastic constants well. A possible defect of potential 3 is the static dielectric constants which we would expect to be larger.

We would like to note that two-body potentials have been used successfully within the shell model to determine phonon modes within these oxide materials.[42–44] These models seem to do a good job of reproducing experimental frequencies and attest to the usefulness of the ionic approach we employ here. Rigid ion models are often used to treat these materials within the ionic description.[46–47] We note that because the shell model produces a coupling with the Buckingham terms, it is not to be expected that a shell-model potential successfully describing a low-symmetry structure can be used within the rigid ion model.

Various impurities have been introduced into the crystal. The potentials used to treat these impurities comes from previous work. The Co^{3+} potentials come from a study of binary oxides.[15,16] The peroxy interaction potential is of the Morse form and comes from an earlier study of La_2CuO_4.[4] Finally, we have used the empirical poten-

TABLE III. Parameters of the potentials. Units of A are eV, ρ are Å, c are eV Å^6, k are eV/Å^2, and k' are eV per degree squared. Values of C are 0.0 unless otherwise noted. The symbol X refers to an oxygen ion at site 1 or 4.

Interaction	Potential 1	Potential 2	Potential 3
	Potentials parameters		
Cu-O, A	3799.3	627.9	712.8
ρ	0.24 273	0.33 501	0.32 698
O-O, A	22 764.0	22 764.0	22 764.0
ρ	0.1490	0.1490	0.1490
C	75.0	75.0	75.0
Ba-O, A	1253.2	1901.3	1644.1
ρ	0.3734	0.35 806	0.35 928
Y-O, A	1123.0	1073.5	1010.3
ρ	0.36 475	0.36 683	0.37 129
Ba-Cu, A	932.5	5653.67	11 552.4
ρ	0.35 031	0.31 348	0.29 373
Cu-X, A	1166.1	3301.4	4817.9
ρ	0.28 871	0.23 693	0.22 432
Ba-X, A	29 194.2	1040.1	1294.7
ρ	0.24 823	0.36 310	0.34 806
X-X, A	22 764.0	22 764.0	22 764.0
ρ	0.1490	0.1490	0.1490
C	75.0	0.0	0.0
	Shell-model parameters		
Y^{3+}, Y	3.0	3.0	3.0
k	999 999.0	999 999.0	999 999.0
Ba^{2+}, Y	9.12	9.12	9.12
k	200.0	426.1	426.1
Cu^{2+}, Y	2.0	2.0	2.0
k	999 999.0	999 999.0	999 999.0
O^{2-}, Y	−3.2576	−3.2576	−3.2576
k	49.8	49.8	49.8
$X^{1.67-}$, Y	−3.2576	−3.2576	−3.2576
k	83.2	100.0	100.0
	Three-body parameters		
∢BaXBa, k'			6.81
θ_0			90.0

[a]Units of A are eV, ρ are Å, c are eV Å^6, k are eV/Å^2, and k' are eV per degree squared. Values of C are 0.0 unless otherwise noted. The symbol X refers to an oxygen ion at site 1 or 4.

tials corrected by electron gas methods[48] to determine short-range potentials for different charge states of copper with oxygen ions.

RESULTS

We begin by a consideration of the energetics of point defect formation. This calculation is performed by removing the appropriate ion from the crystal or substituting, as the case may be, and then allowing complete lattice ion relaxation and polarization to take place. Table IV presents the values which we compute for the processes of vacancy formation or substitution. Generally vacancy formation proceeds with a smaller energy on potentials 2 and 3 (relative to potential 1) where the lattice is softer. Particularly noteworthy is the strikingly lowered oxygen ion vacancy formation at the plane sites. When this energy is compared to the corrected oxygen vacancy energy at the chain this value is smaller. This result is not in agreement with experiment and differs from results for potential 1 and our earlier potential.[6] The vacancy formation energies are combined with the lattice energy to give a Schottky energy which we believe is most reliably given by potential 3 for reasons discussed before. We also consider formation of various copper ion and oxygen ion polaron states at different sites in the crystal. Generally Cu^{3+} is most stable at the Cu(2) site in the plane and Cu^+ is most stable at the Cu(1) site on the chain. The O^- polaron forms most easily at the O(1) chain site in the crystal. The entries in Table IV will be used to compute the energy changes involved in various processes in the crystal through the use of energy cycles[6] in which ions are removed to infinity from the crystal prior to ionization processes and then the resulting species reintroduced into the crystal.

Various models for the defect equilibria in $YBa_2Cu_3O_7$

TABLE IV. Defect energies (eV) computed with different potentials.

	Vacancy Site	Potential 1	Potential 2	Potential 3
	Cu(1)	23.67	22.39	23.98
	Cu(2)	27.92	24.76	25.95
	O(1)	13.69	13.18	14.24
	O(4)	14.35	14.12	15.02
	O(2)	20.37	16.63	17.14
	O(3)	20.17	16.67	17.11
	Ba	17.92	15.13	15.87
	Y	45.49	47.15	47.76
Substitution	Site	Potential 1	Potential 2	Potential 3
O^{2-}	O(5)	−19.81	−19.98	−18.68
Cu^{3+}	Cu(1)	−30.28	−29.32	−29.43
	Cu(2)	−30.98	−29.19	−32.97
Cu^{+}	Cu(1)	17.80	17.06	17.69
	Cu(2)	20.20	20.53	19.56
O^{-}	O(1)	13.38	14.50	14.17
	O(4)	15.05	15.26	14.92
	O(2)	15.13	14.67	13.91
	O(3)	15.11	14.64	13.95
Schottky		30.82	9.81	19.94

have been discussed[26,49,50] involving a variety of species such as Cu^{+}, Cu^{3+}, and O^{-} polarons in addition to the normal lattice ions. These equilibria are related to oxygen content in the crystal through the following possible reactions:

$$\text{Reaction } A\text{: } Cu^{+}+\tfrac{1}{2}O_2+V_0\rightarrow O_0+Cu^{3+}\ ,$$

$$\text{Reaction } B\text{: } 2Cu^{+}+\tfrac{1}{2}O_2+V_0\rightarrow O_0+2Cu^{2+}\ ,$$

$$\text{Reaction } C\text{: } Cu^{+}+\tfrac{1}{2}O_2+V_0\rightarrow O_0'+Cu^{2+}\ , \qquad (3)$$

$$\text{Reaction } D\text{: } 2Cu^{2+}+\tfrac{1}{2}O_2+V_0\rightarrow O_0+2Cu^{3+}\ ,$$

$$\text{Reaction } E\text{: } \tfrac{1}{2}O_2+V_0+O_0\rightarrow 2O_0'\ .$$

In these reactions copper ions in various oxidation states occupy the chain or plane site, the oxygen vacancy is taken at site 1, and O_0' refers to an oxygen ion with -1 charge at site 1. We have constructed energy cycles in order to determine the energy change in each reaction. Here we require the gas-phase electron affinities of oxygen ion and ionization potentials of copper ion to evaluate these terms. The values used here are $E_{EA1}=-1.47$ eV, $E_{EA2}=8.75$ eV, $E_{IP2}=20.39$ eV, and $E_{IP3}=36.83$ eV as employed in earlier work.[4-6] The second electron affinity of oxygen in known with least accuracy and this limits our interpretations of results.

TABLE V. Energy change (eV) of oxidation reactions in $YBa_2Cu_3O_7$. Negative values are exothermic.

Reaction	Copper Ion Site	Potential 2	Potential 3
A	Chain	+3.09	+2.07
B	Chain	−1.10	−2.64
C	Chain	−3.10	−3.55
D	Chain	+7.27	+7.82
	Plane	+7.53	+9.24
E		+4.03	+2.81

The data in Table IV is used to compute the energy change of reactions $A-E$ using potentials 2 and 3. We note that these results presented in Table V correspond to reaction and formation of isolated small polaron species. First consider possible reactions of Cu^{+} by paths $A-C$. The most stable position for this ion is the chain site so only these entries are considered. Clearly reaction *C* leading to a hole on the oxygen ion is the most favorable of these possibilities. Also we note that the direct oxidation of oxide ion via path *E* is least energetically favorable. Our comparisons of reactions $A-D$ are dependent upon parameters such as the electron affinity values discussed above; thus quantitative comparisons need to be taken with caution.

Oxygen may be incorporated in the interstitial sites of the crystal by an addition reaction:

$$\tfrac{1}{2}O_2\rightarrow O_{int}^{2-}+2h^{+}\ . \qquad (4)$$

Our calculations indicate that this reaction is most possible at O site 5 in the crystal and much less possible at the interstitial site next to the planar copper ion. The energy values for oxygen ion vacancy formation versus oxygen ion interstitial formation in Table IV indicate that reaction 4 could replace the oxygen half reactions *A*, *B*, *C*, and *E*.

The diffusion of oxygen ions in the crystal are thought to proceed by a vacancy mechanism. We have sketched some possible mechanisms of diffusion in Fig. 2. We consider the vacancy mechanism for oxygen ion diffusion within the copper-oxygen plane in Fig. 1. Here the sad-

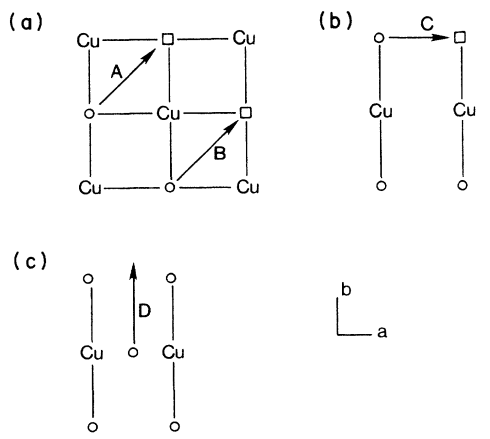

FIG. 2. Sketches of oxygen diffusion mechanisms in $YBa_2Cu_3O_7$. (a) oxygen vacancy in Cu-O plane, (b) oxygen vacancy in chain, (c) oxygen interstitial in chain.

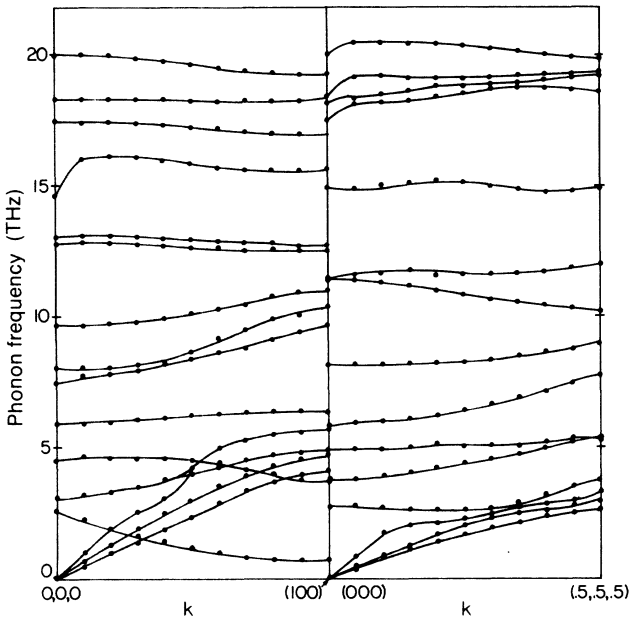

FIG. 3. Computed phonon dispersion curve for $YBa_2Cu_3O_7$ using potential 1.

dle point is computed to be midway between the initial and final configurations. We compute the diffusion energy as the difference in energy between the initial relaxed vacancy configuration and the relaxed saddle-point configuration, and results for the different potentials agree well with one another. There are two possible processes depending upon whether the initial vacancy is on O(2) or O(3) site, and these differ by the corresponding vacancy formation energy in Table IV. Table VI shows that a rather small diffusion energy is found for the O(3) vacancy mechanism in the plane. When we consider the vacancy mechanism in the chain region, as sketched in Fig. 2, the activation energy is computed to be larger for this mechanism in the chain versus the plane. Perhaps this is surprising at first thought because the chain has more open space. However, the saddle point position is stabilized by ion relaxations and polarization which are more effective within the plane. Finally, an interstitial oxygen diffusion mechanism is considered in Fig. 2. The saddle point for this mechanism occurs with the interstitial ion between two oxygen ions. Most of the potentials are unstable for this configuration, but potential 3 is stable and leads to a rather large activation energy. We conclude this mechanism is of minor importance.

Bipolaron species have been discussed within the context of various mechanisms of superconductivity in $YBa_2Cu_3O_7$. We have employed the three-body potential 3 to consider various possibilities such as $(Cu^{3+})_2$, O_2^{2-}, and the charge-transfer species Cu^+O^-. Table VII shows the energy of formation of these bipolaron species computed at various sites in the crystal relative to the individual polaron energies at infinite separation. The O_2^{2-} bipolaron is just unstable by 0.03 eV and this margin is less than the limits of error in our calculation. The most stable O_2^{2-} species forms with the individual O^- unrelaxed positions at O(4),O(2), which means that the axis of this species is about 45° with respect to the crystal c axis. The $(Cu^{3+})_2$ bipolaron is less stable than O_2^{2-} when the polarons are positioned within one bond length of another. Also the possible bipolaron Cu^+Cu^{3+}, which is most stable with the reduced species on Cu(1) and oxidized species on Cu(2), is rather unstable. The charge-transfer species Cu^+O^- is stable with respect to its isolated components. When we construct an energy cycle so as to compute the energy of formation of Cu^+O^- we find the value 5.5 eV for this species within the plane of copper oxide.

We have computed the phonon dispersion curves and eigenfrequencies at $k=0$ for the two-body potentials.

TABLE VI. Activation energy (eV) for oxygen ion diffusion.

Mechanism[a]	Potential 1	Potential 2	Potential 3
A	0.67	0.33	0.31
B	0.47	0.37	0.28
C	2.03	0.62	0.61
D	*XS*[b]	*XS*[b]	2.39

[a] *A* is the planar O(3) vacancy, *B* is the planar O(2) vacancy, *C* is the chain O(1) vacancy, and *D* is the chain O(1) interstitial.

[b] —*XS* core displacement.

TABLE VII. Bipolaron formation energy (eV)—potential 3.

Bipolaron	Structure[a]	E_b (eV)[b]
O_2^{2-}	O(2)O(4)	0.03
O_2^{2-}	O(3)O(4)	0.09
O_2^{2-}	O(2)O(3)	0.15
O_2^{2-}	O(1)O(4)	0.51
$(Cu^{3+})_2$	Cu(2), *a* axis	0.41
$(Cu^{3+})_2$	Cu(2), *b* axis	0.88
$(Cu^{3+})_2$	Cu(1), Cu(2)	1.09
$(Cu^{3+})_2$	Cu(1), *a* axis	0.71
$(Cu^{3+})_2$	Cu(1), *b* axis	1.71
Cu^+O^-	Cu(2), O(2)	−0.06
Cu^+O^-	Cu(2), O(3)	0.29
Cu^+O^-	Cu(2), O(4)	−0.15
Cu^+O^-	Cu(1), O(4)	−0.07
Cu^+O^-	Cu(1), O(1)	−0.15

[a]Nearest-neighbor bipolarons are considered.
[b]Binding energy is relative to separated polarons, negative values are binding.

This is accomplished by solving the equations of motion as discussed earlier using the typhon computer code.[51] Figure 3 is a plot of the phonon dispersion curves for some of the representative optic and acoustic modes of the crystal for potential 1. The only unusual feature in the curves is a softening of a B_{2g} mode which involves a shearing motion of the two copper-oxygen planes. The general features of the phonon dispersion curves have been observed in other experimental and calculated studies.[20,52,53]

The density of states for the phonon dispersion curves of potential 1 is shown in Fig. 4. We have also compared this to a sketch of the experimental curve taken by neutron scattering on a powder sample.[54] The agreement of the two curves is best at low frequencies and becomes poorer at higher frequencies. The good agreement at low frequencies suggests our model provides the best description of the heavier-ion relaxation.

TABLE VIII. Phonon frequencies at $k=0$ for potential 1 (cm^{-1}).

A_g	B_{2g}	B_{3g}	B_{1u}	B_{2u}	B_{3u}
140	72	94	125	107	101
178	150	158	165	153	151
301	328	320	187	199	209
454	367	423	239	289	233
471	613	581	267	340	341
			399	385	376
			529	470	619

The phonon modes at $k=0$ have been analyzed to determine their symmetry in the orthorhombic structure. Table VIII shows the analysis. The *g* modes correspond to Raman active, and the *u* modes correspond to infrared active. Raman frequencies have been computed previously[44] with lattice dynamical models and compared to Raman and infrared experimental absorptions. In some cases the Raman frequencies depend upon the oxygen content of the sample, but experimental A_g Raman modes are reported[44] at 475 cm^{-1}, 435 cm^{-1}, 330 cm^{-1}, and 145 cm^{-1}. A lower-frequency mode due principally to Ba motion has been reported at 116 cm^{-1}. These experimental frequencies may be compared with the data in Table VIII computed and Fig. 5, which shows the major

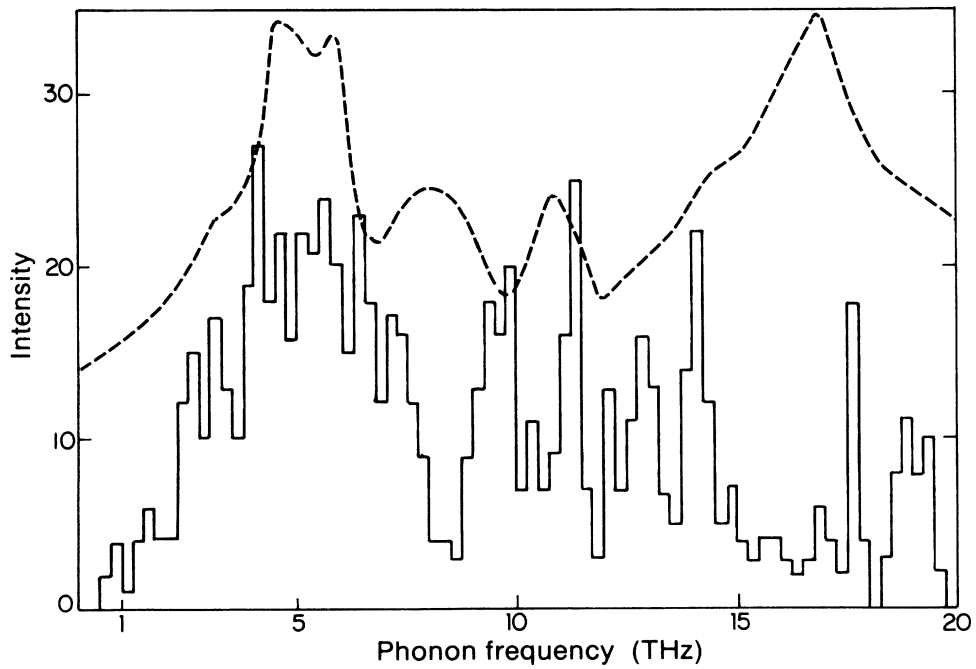

FIG. 4. Density of phonon frequencies (solid line) for potential 1 compared to an experimental study, Ref. 54 (dashed line).

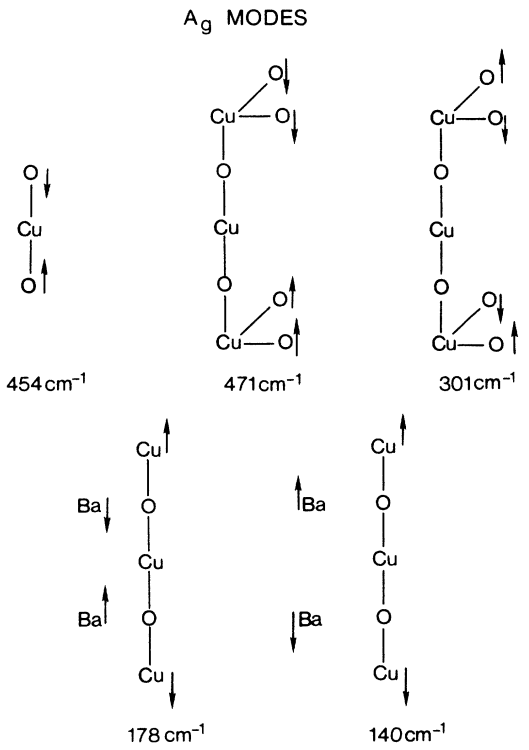

FIG. 5. Sketch of computed A_g phonon modes.

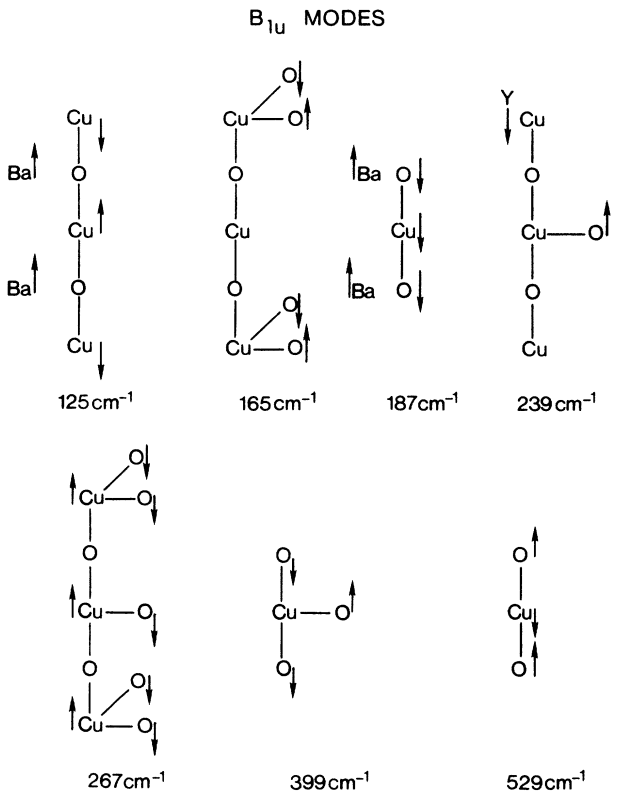

FIG. 6. Sketch of computed B_{1u} phonon modes.

displacements associated with these modes. The previous assignments[42–44] of the Raman frequencies from lattice dynamical calculations are consistent with the data in Fig. 5. In addition to the A_g modes we have also shown the seven computed B_{1u} modes in Fig. 6 which should be infrared active.

Several studies of the phonon frequencies in orthorhombic $YBa_2Cu_3O_7$ have been performed within the framework of the shell model,[42–44] rigid ion model[45] and normal-coordinate calculations.[46] These studies have been able to assign the experimental Raman and infrared frequencies to particular modes with satisfactory agreement often with a 5–10% discrepancy between experiment and theory. Our particular study has also achieved this level of accuracy, although we have taken no particular effort to match theoretical to experimental frequencies. This result supports our approach and gives greater credence to the defect calculations.

Recent extended x-ray-absorption fine structure (EXAFS) experiments[55] have shown evidence for clumping of impurity Co^{3+} ions on the Cu^{2+} chain sites of $YBa_2Cu_3O_7$. Our calculations[6,7] with earlier potentials showed a definite preference for isolated Co^{3+} ions to substitute at the chain Cu^{2+} site with the incorporation of excess oxygen ion. We now wish to examine the possible clumping of Co^{3+} ions and the associated metal-oxygen bond lengths with our improved three-body potential 3. Zig-zag single and double chain structures have been reported and examined in this study. Figure 7 shows the results for single and double chains by substituting Co_4O_6 and Co_7O_{10} for Cu^{2+} ions at the chain. We observe alternations in the Co—O bond length and a range of lengths varying from 1.62–2.48 Å. These values are in the range of experimental data, but there is a considerable spread of the calculated values. Improved po-

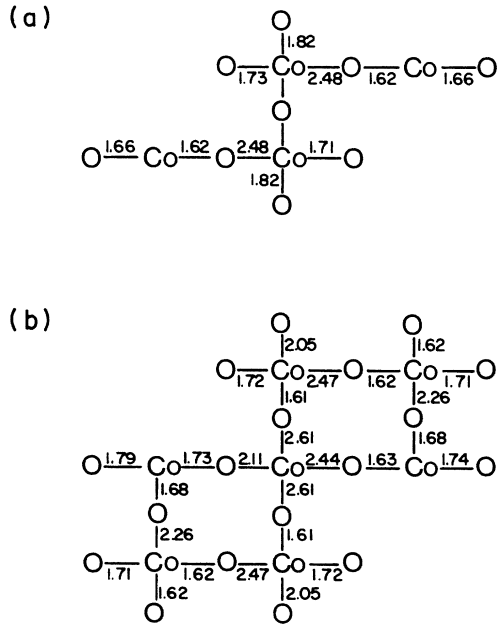

FIG. 7. Sketch of computed relaxed ion positions and bond lengths for Co_4O_6 and Co_7O_{10} using potential 3. A single-chain and double-chain model as proposed in Ref. 55 are considered.

tentials for the impurity may be needed along with a supercell type approach to better examine these complete impurity phases. At the present level of calculation we only wish to emphasize the appearance of alternating bond lengths.

DISCUSSION

We have shown that the structure and physical properties of $YBa_2Cu_3O_7$ may be simulated well by the atomistic model. Two-body terms seem to be sufficient in matching the structure, but three-body terms are important in giving good elastic constants. Our prior experience has shown that the two-body potentials give reliable information on the relaxations and polarization surrounding defect formation[6] and the systematics of impurity substitution.[7] The present work also gives phonon dispersion results and frequencies which can be sensibly compared to the corresponding experiment. All of this supports the reliability of the atomistic model description of $YBa_2Cu_3O_7$.

We attach the greatest quantitative reliability to the three-body potential 3 results. However, oxygen vacancy formation is easiest at the plane site which is not in agreement with experiment.[56] The Schottky energy of 19.94 eV corresponds to 1.53 eV per vacancy which should be expected near the oxygen stoichiometry of seven. The finding that Cu(1) site prefers the reduced copper ion and that the Cu(2) site prefers the oxidized copper ion is consistent with chemical ideas based upon the number of copper-oxygen bonds.

We may consider the oxidation reactions reported in Table V. These reactions are for isolated defects and it is therefore difficult to compare to experimental enthalpies[26] which correspond to formation of extended regions of the oxidized species. Additionally our conclusions depend upon the experimental electron affinity values of oxygen which involve some uncertainty. We can conclude that the direct oxidation of oxide ions by oxygen (reaction *E*) can be excluded and that reaction *C* involving lattice Cu^+ would be required to form the O^- species in the crystal. The energy of this reaction is exothermic, but here the oxygen electron affinity value plays an important role. Oxidation of Cu^+ (reaction *C*) is the most favorable oxidation reactions involving copper ions. It is consistently found that the most favorable oxidation reaction involving copper ions takes place on the planes and not the chains. Finally we note that the oxidation of Cu^+ (reaction *C*) has been proposed[49] from experimental conductivity and thermopower data. This result and our calculations seen to be mutually consistent.

The diffusion of oxygen ions in $YBa_2Cu_3O_7$ has been measured by resistivity. The activation energy of motion was deduced to be 0.48 eV from the measurements.[24,25] Arrhenius plots yielded an activation energy of 0.40 eV in other experimental studies,[23] but the mechanism was not discussed. Our data in Table VI suggest that the activation energy for motion seems to agree well with these experimental data. This may be an oversimplification of the experimental situation, since other measurements[57] are interpreted to give a larger activation energy of 0.97 eV. The smallest activation energy occurs in the copper-oxygen plane and involves a vacancy mechanism. The vacancy mechanism in the chain has a higher activation energy and interstitial diffusion mechanisms do not seen likely.

EXAFS measurements[55] of Co^{3+} substituted for copper ions in $YBa_2Cu_3O_7$ show substitution to occur at the chain site. Evidence for two Co—O bond lengths of 1.8 and 2.4 Å led to the proposal of zig-zag single and double chains as possible arrangements for the cobalt ions. Our calculations definitely support the idea of long and short cobalt-oxygen bond lengths. The shortest bond length which we compute is 1.62 Å, but many of the bonds have values near 1.8 Å in either the double or single chain structure.

We may consider the relative stabilities of small versus large polarons in $YBa_2Cu_3O_7$. This approximate calculation is based upon the difference in energy between a thermal and optical calculation for a particular defect. The thermal calculation allows full core and shell relaxations and ion relations according to the procedure we have discussed earlier. In the optical calculation the cores are frozen in position so that only electronic polarization is allowed. The difference in energy of the two calculations represents the component due to ion relaxations or the polaron field. This difference should be compared to half the valence bandwidth to determine whether the small or large polaron is more stable. Table IX contains this difference for copper ion and oxygen ion polarons. An estimate of half the valence bandwidth is 3 eV from photoemission spectra.[58] The valence bandwidth is a complex mixture of copper ion *d* states and oxygen ion *p* states so that it is difficult to determine the half-bandwidth value for each of these separate ions, but the value is less than 3 eV. The entries of potential 3 in Table IX support the small polaron model for Cu^{3+} and O^- at several sites. There may be some cases where the large polaron is favored.

Bipolarons have been discussed in various superconductivity mechanisms in the copper oxide systems. These have included mechanisms with small bipolarons[12,13,59,60] or large bipolarons. The small bipolaron consists of two bound small polarons each in the form of an ion with extra charge and its associated field of relaxed and polarized lattice ions. This mechanism has been applied to examine possible conduction mechanisms involving Cu^{3+} or Cu^+/Cu^{3+} disproportionated chains. The possibility

TABLE IX. Difference of thermal and optical defect energy (eV)—potential 3.

Defect	Site	Energy (eV)
Cu^{3+}	Cu(1)	3.02
Cu^{3+}	Cu(2)	4.58
Cu^+	Cu(1)	2.44
Cu^+	Cu(2)	1.78
O^-	O(1)	3.57
O^-	O(4)	2.55
O^-	O(2)	3.13
O^-	O(3)	3.08

of large bipolarons[61,62] forming a basis for superconductivity has been based on the point that they could be quite mobile. It is shown that if $\epsilon_0 \gg 2\epsilon_\infty$ a bound large bipolaron could exist and that the copper oxide systems should obey this relationship in terms of the dielectric constants. Note that the computed dielectric constants in Table II obey this relationship.

We do not find evidence for the formation of Cu^{3+} small bipolarons. The binding energy terms in Table VII indicate that such a species is unstable by at least a few tenths of an eV. The O_2^{2-} species has a much greater chance of being observed in the crystal. In earlier calculations for the peroxy type of bipolaron in La_2CuO_4 (Ref. 5) was found to be stable. The peroxiton species determined in other work[63,64] may be compared to the O_2^{2-} species. We note that stability of this species is observed for geometries where the O(4) ion interacts with one of the oxygen ions in the plane. The charge-transfer Cu^+O^- bipolaron is generally bound with respect to the isolated polarons. When the energy is computed relative to doubly charged copper and oxygen ions slightly more than 5 eV is required to form this species. We note that experimental evidence for polarons or bipolarons in $YBa_2Cu_3O_7$ has been recently reported.[65]

Models involving double potential wells[66-68] have been discussed as enhancing electron-phonon coupling in various mechanisms of superconductivity. These models involve displacements of the O(1) oxygen ion in the a direction, the Ba^{2+} ions in the c direction or possible movements of copper ion polaron states along the c axis. We have examined these possibilities with potential 1 and 3 to determine whether any double wells could be found. None have been found for any of these motions involving O(1) or Ba ions. We have extensively examined the symmetric and antisymmetric motions of two Cu^{3+} polaron species in adjacent copper oxide planes along the c axis and did not find double minima. This could be due to some artifacts in our potential models or possibly a more complex motion is necessary to find the double minimum.

SUMMARY

This work has shown that two- and three-body formulations of short-range interactions plus the shell-model fit the elastic constants and structure of $YBa_2Cu_3O_7$ well. Several potential models were examined with various distributions of formal charge to lead to the present model with one hole per three oxygen ions attached to chain copper ion. The present model is fit to experimental elastic constants which have a smaller value than used in our earlier work.[6] Thus the lattice is softer and vacancy formation energies become smaller. We compute the Schottky energy to be 19.94 eV.

Various solid-state redox reactions involving the incorporation of O(2) in the crystal are considered. The energetics of these reactions are exothermic for oxidation of Cu^+, Cu^{2+}, or O^{2-}. Comparison of various different reactions on a quantitative basis is difficult because of the need of the oxygen ion second electron affinity which is known only with some uncertainty. Nevertheless the reaction

$$Cu^+ + \tfrac{1}{2}O_2 + V_0 \rightarrow O_0' + Cu^{2+} \tag{5}$$

appears quite possible for isolated polaron species.

Diffusion of oxygen ions in the structure is considered using the vacancy and interstitial mechanisms. The vacancy mechanism is most favorable when it occurs in the Cu-O plane and gives an activation energy of about 0.3 eV. This compares well with experimental values of about 0.4 eV.

The phonon frequencies are computed from the equations of motion. Comparison of the computed density of frequencies to experimental data gives good agreement at low frequencies and some deviation at higher frequency. The frequencies at $k=0$ compare well with the Raman experimental frequencies.

Various bipolaron species such as $(Cu^{3+})_2$, O_2^{2-}, and Cu^+O^- are considered. The Cu^{3+} species is unstable by several tenths of an eV and is not considered likely. The O_2^{2-} species is unibound by only 0.03 eV which is within the limits of our calculation and parameters and is considered a likely possibility in this crystal. The Cu^+O^- species is found with respect to the isolated species, but requires just in excess of 5 eV to be formed.

A simulation of chains of Co^{3+} substituted for Cu^{2+} is performed. We find that there is an alternation in value of Co—O bond length as found in experiment. Excess oxygen is incorporated with Co^{3+} as part of the compensation mechanism.

The potentials developed in this work seem to give good representations of many properties of orthorhombic $YBa_2Cu_3O_7$. Of course the potentials can be improved as more data becomes available for the crystal. In the meantime these can be expected to perform well in describing a range of crystal properties.

[1]C. N. R. Rao and B. Raveau, Acc. Chem. Res. **22**, 106 (1989).
[2]T. V. Ramakrishnan and C. N. R. Rao, J. Phys. Chem. **93**, 4414 (1989).
[3]J. A. Wilson, J. Phys. C **21**, 2067 (1988).
[4]M. S. Islam, M. Leslie, S. M. Tomlinson, and C. R. A. Catlow, J. Phys. C **21**, L109 (1988).
[5]C. R. A. Catlow, S. M. Tomlinson, M. S. Islam, and M. Leslie, J. Phys. C **21**, L1085 (1988).
[6]R. C. Baetzold, Phys. Rev. B **38**, 11 304 (1988).
[7]M. S. Islam and R. C. Baetzold, Phys. Rev. B **40**, 10 926 (1989).
[8]N. L. Allan and W. C. Mackrodt, Philos. Mag. A **58**, 555 (1988).
[9]N. L. Allan, J. M. Lawton, and W. C. Mackrodt, J. Phys. C **1**, 2657 (1989).
[10]W. C. Mackrodt, Supercon. Sci. Technol. **1**, 343 (1989).
[11]R. J. Birgeneau, C. Y. Chen, D. R. Gabbe, H. P. Jenssen, M. A. Kastner, C J. Peters, P. J. Picone, T. Thio, T. R. Thurston, H. L. Tuller, J. D. Axe, P. Boni, and G. Shirane, Phys. Rev. Lett. **59**, 1329 (1987).
[12]L. J. deJongh, Physica C **152**, 171 (1988).

[13]L. J. deJongh, Solid State Commun. **65**, 963 (1988).
[14]F. Beech, S. Miraglia, A. Santoro, and R. S. Roth, Phys. Rev. B **35**, 8778 (1987).
[15]G. V. Lewis and C. R. A. Catlow, J. Phys. Chem. Solids **47**, 89 (1986).
[16]G. V. Lewis and C. R. A. Catlow, J. Phys. C **18**, 1149 (1985).
[17]W. C. Mackrodt and R. F. Stewart, J. Phys. C **12**, 431 (1979).
[18]A. M. Stoneham and J. R. Harding, Annu. Rev. Phys. Chem. **37**, 53 (1986).
[19]P. Baumgart, S. Blumemroder, A. Erle, B. Hillebrands, G. Guntherodt, and H. Schmidt, Solid State Commun. **69**, 1135 (1989).
[20]W. Reichardt, L. Pintschovius, B. Hennion, and F. Collin, Supercond. Sci. Technol. **1**, 173 (1988).
[21]D. J. Werder, C. H. Chen, R. J. Cava, and B. Batlogg, Phys. Rev. B **37**, 2317 (1988).
[22]B. Batlogg and R. J. Cava, Physica B **148**, 173 (1987).
[23]G. Ottaviani, C. Nobili, F. Nava, M. Affronte, T. Manfredini, F. C. Matacotta, and E. Galli, Phys. Rev. B **39**, 9069 (1989).
[24]K. N. Tu, C. C. Tsuei, S. I. Park, and A. Levi, Phys. Rev. B **38**, 772 (1988).
[25]K. N. Tu, N. C. Yeh, S. I. Park, and C. C. Tsuei, Phys. Rev. B **39**, 304 (1989).
[26]M. E. Parks, A. Narrotsky, K. M. Mocalla, E. Takayama-Maromachi, A. Jocaoson, and P. K. Davies, J. Solid State Chem. **79**, 53 (1989).
[27]See *Computer Simulation of Solids,* Vol. 166 of *Lecture Notes in Physics,* edited by C. R. A. Catlow and W. C. Mackrodt (Springer-Verlag, Berlin, 1982).
[28]C. R. Catlow, Annu. Rev. Mater. Sci. **16**, 517 (1986).
[29]B. G. Dick and A. W. Overhauser, Phys. Rev. **112**, 90 (1958).
[30]N. F. Mott and M. J. Littleton, Trans. Faraday Soc. **34**, 485 (1938).
[31]M. J. Norgett, Atomic Energy Research Establishment Report No. R7650, 1974 (unpublished).
[32]M. Leslie, Science and Engineering Research Council, Daresbury Laboratory, England.
[33]R. C. Baetzold, Inorg. Chem. **28**, 640 (1989).
[34]R. G. Gordon and Y. S. Kim, J. Chem. Phys. **56**, 3122 (1972); **60**, 1842 (1974).
[35]D. J. Bishop, A. P. Ramirez, P. L. Gammel, B. Batlogg, E. A. Rietman, R. J. Cava, and A. J. Millis, Phys. Rev. B **36**, 2408 (1987).
[36]H. M. Ledbetter, M. W. Ausiton, S. A. Kim, and M. Lei, J. Mater. Res. **2**, 786 (1987).
[37]M. Cankurtaran, G. A. Saunders, J. R. Willis, A. Ad-Kheffaji, and D. P. Almond, Phys. Rev. B **39**, 2872 (1989).
[38]M. Saint-Paul, J. L. Tholence, P. Monceau, N. Noel, J. C. Levet, M. Potel, P. Gougeon, and J. J. Capponi, Solid State Commun. **66**, 641 (1988).
[39]H. Ledbetter and M. Lei (unpublished).
[40]W. H. Fietz, M. R. Dietrich, and J. Euke, Z. Phys. B **69**, 17 (1987).
[41]C. R. A. Catlow, C. M. Freeman, and R. L. Royle, Physica B **131**, 1 (1985).
[42]W. Kress, U. Schroder, J. Prade, A. D. Kulkarni, and F. W. deWette, Phys. Rev. B **38**, 2906 (1988).
[43]C. Thomsen, M. Cardona, W. Kress, R. Liu, L. Genzel, M. Bauer, E. Schonherr, and U. Schroder, Solid State Commun. **65**, 1139 (1988).
[44]R. Liu, C. Thomsen, W. Kress, M. Cardona, B. Gegenheimer, F. W. deWette, J. Prade, A. D. Kulkarni, and U. Schroder, Phys. Rev. B **37**, 7971 (1988).
[45]F. E. Bates, Phys. Rev. B **39**, 322 (1989).
[46]P. A. Deymier, Phys. Rev. B **38**, 6596 (1988).
[47]D. P. Billesbach, J. R. Hardy, and P. J. Edwardson, Phys. Rev. B **39**, 202 (1989).
[48]V. Butler, C. R. A. Catlow, B. E. F. Fender, and J. H. Harding, Solid State Ionics **8**, 109 (1983).
[49]M.-Y. Su, S. E. Dorris, and T. O. Mason, J. Solid State Chem. **75**, 381 (1988).
[50]G. M. Choi, H. L. Tuller, and M.-J. Tsai, in *Non-Stoichiometric Compounds Surfaces, Grain Boundaries and Sturtural Defects,* edited by J. Nowotny and W. Weppner, (Kluwer Academic, Dordrecht, (1989).
[51]Typhon Code of M. J. L. Sangster and D. K. Rowell, Atomic Energy Research Establishment, Harwell, England.
[52]S. Mase, T. Yasuda, Y. Horie, and T. Fukami, Solid State Commun. **65**, 477 (1988).
[53]S. Mase, T. Yasuda, Y. Horie, M. Kusaba, and T. Fukami, J. Jpn. Phys. Soc. **57**, 1024 (1988).
[54]J. J. Rhyne, D. A. Neumann, J A. Gotaas, F. Beech, L. Toth, S. Lawrence, S. Wolf, M. Osofsky, and D. U. Gubser, Phys. Rev. B **36**, 2294 (1987).
[55]F. Bridges, J. B. Boyce, T. Claeson, T. H. Geballe, and J. M. Tarascon, Phys. Rev. B **39**, 11 603 (1989).
[56]I. K. Schuller, D. G. Hinks, M. A. Beno, D. W. Capone II, L. Scoderholm, J.-P. Lacquet, Y. Bruynserade, C. U. Segre, and K. Zhany, Solid State Commun. **63**, 385 (1987).
[57]S. J. Rothman, J. L. Routbort, and J. E. Baker, Phys. Rev. B **40**, 8852 (1989).
[58]A. J. Arko, R. S. List, R. J. Bartlett, S.-W. Cheong, Z. Fisk, J. D. Thompson, C. G. Olson, A.-B. Yang, R. Liu, C. Gu, B. W. Veal, J. Z. Liu, A. P. Paulikas, K. Vandervoort, H. Claus, J. C. Campuzano, J. E. Schirber, and N. D. Shinn, Phys. Rev. B **40**, 2268 (1989).
[59]L. J. deJongh, Physica C **153**, 214 (1988).
[60]L. J. deJongh, J. Chim. Phys. **85**, 1105 (1988).
[61]D. Emin, Phys. Rev. Lett. **62**, 1544 (1989).
[62]D. Emin and M. S. Hillery, Phys. Rev. B **39**, 6575 (1989).
[63]B. K. Chakroverty, D. Feinberg, Z. Hang, and M. Avignon, Solid State Commun. **64**, 1147 (1987).
[64]B. K. Chakroverty, D. D. Sarma, and C. N. R. Rao, Physica C **156**, 413 (1988).
[65]Y. H. Kim, C. M. Foster, A. J. Heeger, S. Cox, and G. Stucky, Phys. Rev. B **38**, 6478 (1988).
[66]R. M. Martin (private communication).
[67]J. R. Hardy and F. W. Flocken, Phys. Rev. Lett. **60**, 2191 (1988).
[68]J. C. Phillips, *Physics of High T_c Superconductors* (Academic, Boston, 1989).